

Search for anomalous couplings via single top quark production in association with a photon at LHC

Yu-Chen Guo ¹, Chong-Xing Yue ^{1,*} and Shuo Yang ²

¹ *Department of Physics, Liaoning Normal University, Dalian 116029, China*

² *Physics Department, Dalian University, Dalian 116622, China*

Abstract

Considering the experimental constraints given by CMS collaboration at $\sqrt{s} = 8$ TeV on the strength of top quark flavour-changing neutral-current (FCNC) couplings $tq\gamma$ and tqg , we investigate the production of top quark in association with a photon and carry out a full simulation for the signals γjjb and $\gamma \ell \nu b$ at LHC-RunII. In our numerical analysis, the contributions of single top production with a photon radiation off the top decay products are also included. The discovery potential for anomalous couplings $tq\gamma$ and tqg at LHC-RunII with 100 fb^{-1} are examined in detail.

*Electronic address: cxyue@lnmu.edu.cn

I. INTRODUCTION

The top quark is generally considered as a sensitive probe to physics beyond the standard model (BSM)[1], with its large mass close to the electroweak symmetry breaking scale. Transitions between top quarks and other quark flavours mediated by neutral gauge bosons, the flavour-changing neutral-currents (FCNC), are forbidden at tree level in the Standard Model (SM) and suppressed at the level of quantum loop due to the Glashow-Iliopoulos-Maiani (GIM) mechanism[2]. The branching ratios for the processes $t \rightarrow q\gamma$ and $t \rightarrow qg$ are of the order of $10^{-14} - 10^{-12}$ in the SM [3, 4]. In contrast, several BSM scenarios, such as the two-Higgs doublet model, supersymmetry or technicolor, predict much larger rates [5, 6] of the order of $10^{-6} - 10^{-5}$. It implies that observation of the large FCNC-induced couplings $tq\gamma$ and tqg would indicate the existence of BSM.

The enhanced FCNC $tq\gamma$ and tqg interactions are predicted by many extensions of the SM which include new exotic quarks [7], new scalars [8, 9], supersymmetry [5, 10–14], or technicolour [6, 15]. The BSM effects can be described by a minimal set of the higher order effective operators independently from the underlying theory [16]. The effective operators not only simplify multiple free parameters of specific models in a model-independent way, but also order them and allow us to consistently take into account higher-order quantum corrections. This method appears in many studies to search top-quark FCNC [17–37]. It can facilitate the analysis of new physics effects in $tq\gamma$ and tqg interactions. So we can give limits on the strength of anomalous top couplings in a model-independent way. The most general effective Lagrangian can be written as

$$\begin{aligned}
 \mathcal{L}_{eff} = & - eQ_t\bar{u}\frac{i\sigma^{\mu\nu}q_\nu}{\Lambda}(\kappa_{tu\gamma}^L P_L + \kappa_{tu\gamma}^R P_R)tA_\mu \\
 & - eQ_t\bar{c}\frac{i\sigma^{\mu\nu}q_\nu}{\Lambda}(\kappa_{tc\gamma}^L P_L + \kappa_{tc\gamma}^R P_R)tA_\mu \\
 & - g_s\bar{u}\frac{i\sigma^{\mu\nu}q_\nu}{\Lambda}(\kappa_{tug}^L P_L + \kappa_{tug}^R P_R)T^a tG_{a\mu} \\
 & - g_s\bar{c}\frac{i\sigma^{\mu\nu}q_\nu}{\Lambda}(\kappa_{tcg}^L P_L + \kappa_{tcg}^R P_R)T^a tG_{a\mu} + h.c., \tag{1}
 \end{aligned}$$

where Q_t is the electric charge of the top quark, g_s is the strong-coupling constant, $T^a = \lambda_a/2$ are color matrices, q is the momentum of the gauge boson, and $P_{L(R)}$ denotes the left(right)-handed projection operators. Λ is the new physics scale, which is related to the cutoff mass scale above which the effective theory breaks down. The terms with

$\sigma^{\mu\nu} = \frac{1}{2}[\gamma^\mu, \gamma^\nu]$ are suppressed by the GIM mechanism, and in consequence are absent at tree-level in renormalizable theories, like the SM. Real dimensionless parameters $\kappa_{tqV}^{L,R}$ are the strength of anomalous couplings tqV with $V = \gamma, g$ and $q = u, c$.

Among FCNC top quark decays, $t \rightarrow qg$ is very difficult to distinguish from generic multijet production via quantum chromodynamics (QCD). It has therefore been suggested to search for FCNC couplings in anomalous single top-quark production. The existence of anomalous couplings $tq\gamma$ and tqg would induce production of a top quark in association with a photon, $pp \rightarrow t\gamma + X$. Next-to-leading order QCD predictions for this process have been studied in [24, 33]. This process has been probed at the CMS experiment, as yet, with no indication of any signal. The stronger bounds on the strengths of anomalous couplings have been provided by the LHC experiments with $\sqrt{s} = 8$ TeV [38, 39]. We use the CMS results and try to predict the discovery potential of LHC-RunII.

The aim of this paper is to investigate the limits on anomalous top couplings by considering $t\gamma$ production. Unlike previous studies of $t\gamma$ production, we focus on a detailed analysis based on the complete simulation. In addition, we discuss the sensitivity of LHC-RunII to anomalous top couplings and detection potential lower limits on the $tq\gamma$ and tqg couplings.

The rest of the paper is organized as follows. In Section II, we provide the cross sections of $t\gamma$ production at LHC-RunII. The simulation of signal and the expected backgrounds is discussed in detail. At the end of this section, we discuss the contribution of single top production with a photon radiation off the top decay products. In section III, we analyze the sensitivity of LHC-RunII to anomalous top couplings in detail. The limits on the branching ratios of top quarks into lighter quarks and photons or gluons are given correspondingly. Finally we summarize our results in section IV.

II. ANOMALOUS TOP COUPLINGS AND $t\gamma$ PRODUCTION AT LHC

In this section we first study $t\gamma$ production with the on-shell top quark in the final state, and then discuss the signal and background events for two channels γjjb and $\gamma \ell \nu b$ depending on the W decay mode. A realistic and detailed analysis is presented, including object identification and event selection.

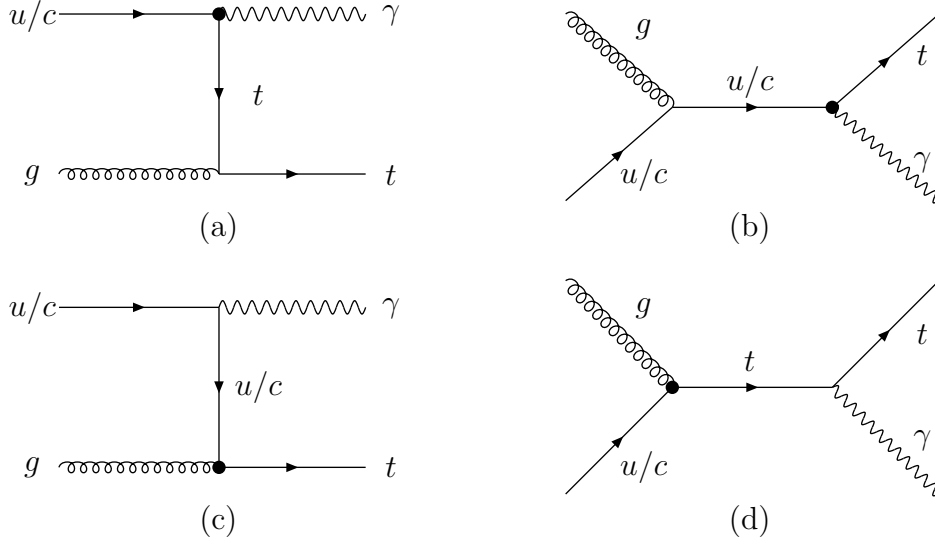


FIG. 1: Leading order Feynman diagrams for anomalous $t\gamma$ production. Flavor violation (the dots) occurs either in the weak (a,b) or strong (c,d) sector.

A. $t\gamma$ production

From the general effective Lagrangian \mathcal{L}_{eff} as shown in Eq.(1), one can see that anomalous couplings $tq\gamma$ and tqg induce the process $pp \rightarrow t\gamma$. The $t\gamma$ production provides the opportunity to probe both anomalous tuV and tcV couplings. Less sensitivity to tcV couplings is expected due to the large enhancement of the charm quark parton distribution function (PDF). Therefore, we consider that each type of interaction, $tu\gamma$, $tc\gamma$ and tug , tcg , should be treated independently. In our analysis, we take Λ as the top quark mass, $m_t = 173.2$ GeV, $\alpha_s = 0.108$, $\alpha = 1/128.92$ and a simplified scenario with $\kappa_{tq\gamma}^L = \kappa_{tq\gamma}^R = \kappa_{tq\gamma}$ and $\kappa_{tqg}^L = \kappa_{tqg}^R = \kappa_{tqg}$.

The presence of anomalous couplings $tq\gamma$ and tqg lead to the single top production in association with an energetic photon by two main mechanisms related to the strong and weak sector. This process can take place through the s- and t-channel. The corresponding Feynman diagrams are shown in Fig. 1. The effective cross sections $\sigma(s)$ can be evaluated from $\hat{\sigma}(\hat{s})$ by convoluting with $f_{q_1/p}(x_1)$ and $f_{q_2/p}(x_2)$,

$$\sigma(s) = \int_{x_{min}}^1 dx_1 \int_{x_{min}/x_1}^1 dx_2 f_{q_1/p}(x_1) f_{q_2/p}(x_2) \hat{\sigma}(\hat{s}), \quad (2)$$

where $\hat{s} = x_1 x_2 s$ is the effective center-of-mass (c. m.) energy squared for the partonic

process, and $x_{min} = m_t^2/s$. For the quark distribution functions $f_{q1/p}(x_1)$ and $f_{q2/p}(x_2)$, we will use the form given by the leading order parton distribution function CTEQ6L1 [40].

The effective Lagrangian is implemented in FeynRules [41] and subsequently passed to MadGraph 5 [42] framework by means of UFO module [43]. We assume that only one anomalous top coupling is nonzero. It is worth mentioning that if the photon is collinear to the initial quark, the cross section will have a divergence. To avoid this divergence, we set a minimum transverse momentum cut on emitted photons, $p_T^\gamma > 50$ GeV which is adopted by CMS collaboration. In this case, the $t\gamma$ cross section for LHC-RunII are

$$\begin{aligned}
\sigma_{t\gamma}(\kappa_{tu\gamma}) &= 144.4 |\kappa_{tu\gamma}|^2 (pb) , \\
\sigma_{t\gamma}(\kappa_{tc\gamma}) &= 13.7 |\kappa_{tc\gamma}|^2 (pb) , \\
\sigma_{t\gamma}(\kappa_{tug}) &= 401.6 |\kappa_{tug}|^2 (pb) , \\
\sigma_{t\gamma}(\kappa_{tcg}) &= 55.7 |\kappa_{tcg}|^2 (pb) .
\end{aligned}
\tag{3}$$

Obviously, the cross sections of $t\gamma$ production only depend on the strengths of anomalous top couplings $\kappa_{tq\gamma}$ and κ_{tqg} .

There are many alternatives for normalisation of coupling constants in \mathcal{L}_{eff} . The experimental results always use branching ratios. In order to compare with them, we will show our results by using branching ratios of top quark. In our analysis, the width of $t \rightarrow Wb$ is assumed to be approximately top quark total width. The LO prediction for decay width of top quark decay to a bottom quark and a W boson is [44]

$$\Gamma(t \rightarrow Wb) = \frac{\alpha}{16s_w^2} |V_{tb}|^2 \frac{m_t^3}{m_W^2} \left[1 - 3 \frac{m_t^4}{m_W^4} + 2 \frac{m_t^6}{m_W^6} \right].
\tag{4}$$

The partial widths of the top FCNC decays $t \rightarrow q\gamma$ and $t \rightarrow qg$ are expressed as follows

$$\begin{aligned}
\Gamma(t \rightarrow q\gamma) &= \frac{2\alpha}{9} m_t^3 \frac{|\kappa_{q\gamma}|^2}{\Lambda^2}, \\
\Gamma(t \rightarrow qg) &= \frac{2\alpha_s}{3} m_t^3 \frac{|\kappa_{qg}|^2}{\Lambda^2}.
\end{aligned}
\tag{5}$$

We plot the cross section of $t\gamma$ production at LHC-RunII originating from different anomalous couplings tqV versus the FCNC branching ratios in Fig.2. From Fig.2, we can see that the cross sections of anomalous $t\gamma$ production increase with the FCNC branching

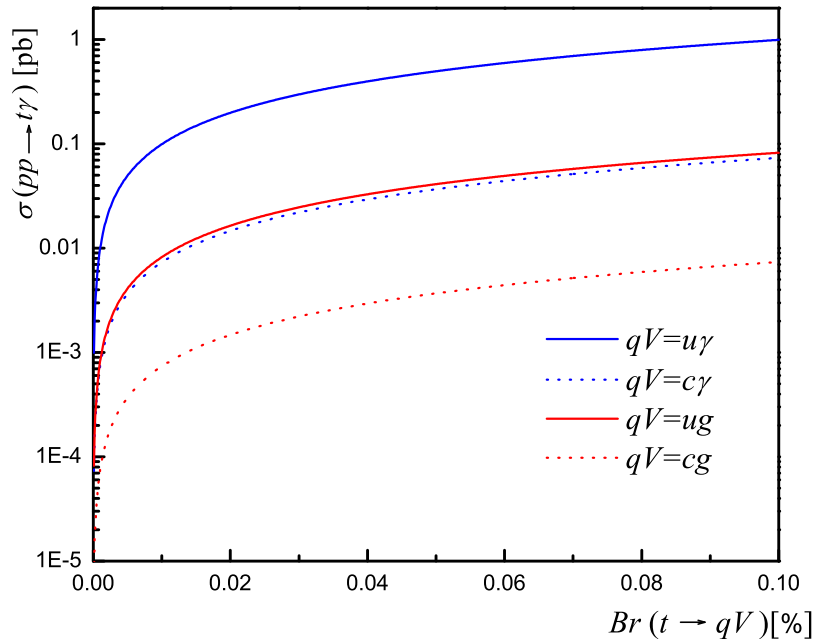


FIG. 2: The cross sections of anomalous $t\gamma$ production versus the FCNC branching ratios $\mathcal{BR}(t \rightarrow u\gamma)$, $\mathcal{BR}(t \rightarrow c\gamma)$, $\mathcal{BR}(t \rightarrow ug)$ and $\mathcal{BR}(t \rightarrow cg)$.

ratios increasing. Experimental limits on the branching ratios of the rare top quark decays were established by experiments of top production at the LEP, HERA, Tevatron and LHC accelerators [38, 39, 45–50]. At present the most stringent upper limits at 95% confidence level (CL) from different sensitive channels are shown in Table I. Using the upper limits on the branching ratios by the CMS experiment,

$$\mathcal{BR}(t \rightarrow u\gamma) < 1.61 \times 10^{-4}, \quad \mathcal{BR}(t \rightarrow c\gamma) < 1.82 \times 10^{-3}, \quad (6)$$

$$\mathcal{BR}(t \rightarrow ug) < 3.55 \times 10^{-4}, \quad \mathcal{BR}(t \rightarrow cg) < 3.44 \times 10^{-3}, \quad (7)$$

we obtain the limits on the cross section in Fig.2. Then we use Eq.3 to calculate the strengths of anomalous top couplings

$$\kappa_{tu\gamma} < 0.028, \quad \kappa_{tc\gamma} < 0.094, \quad \kappa_{tug} < 0.036, \quad \kappa_{tcg} < 0.112, \quad (8)$$

which are coincident with that given by [38, 39].

TABLE I: The most stringent experimental upper bounds on the top quark FCNC branching ratios at 95% CL obtained in CDF, D0, ATLAS and CMS from different channels.

EXP	\sqrt{s} TeV	$\mathcal{L}(\text{fb}^{-1})$	\mathcal{BR}	$(q = u)\%$	$(q = c)\%$	Ref
CDF	1.8	0.11	$t \rightarrow q\gamma$	3.2		[45]
CMS	8	19.1		0.0161	0.182	[38]
CDF	1.96	2.2	$t \rightarrow qg$	0.039	0.57	[46]
D0	1.96	2.3		0.02	0.39	[47]
CMS	7	4.9		0.56	7.12	[48]
CMS	7	4.9		0.035	0.34	[39]
ATLAS	8	14.2		0.0031	0.016	[49]

B. Signal and background simulation

Different decay channels of W give different experimental signals. There are two kinds of signals, γjjb and $\gamma \ell \nu b$.

$$pp \rightarrow t\gamma \rightarrow W^+ b\gamma \rightarrow jjb\gamma, \quad (9)$$

and

$$pp \rightarrow t\gamma \rightarrow W^+ b\gamma \rightarrow \ell \nu b\gamma. \quad (10)$$

For numerical estimation, we take coupling constants $\kappa_{tu\gamma} = 0.001$, $\kappa_{tc\gamma} = 0.003$, $\kappa_{tug} = 0.01$ and $\kappa_{tcg} = 0.02$ in the following signal simulation.

The light jet would be misidentified as b -jet (or photon) candidate and therefore $W\gamma$ +jets events will be one of backgrounds with a fake b -jet. Similarly, W +jets will contribute to backgrounds if two jets are misidentified as an isolated photon and a b -jet simultaneously, respectively. For the background events with more than one b -jet (such as $t\bar{t}$, $t\bar{t} + \gamma$ events), we only take into account $t\bar{t}$ because of its large cross section at LHC. The measurement accuracy of the hadronic calorimeter is not enough to distinguish the W or Z boson. Thereby, $Z\gamma$ +jets process contributes to backgrounds, which is larger than others SM background processes such as single top+ γ , $t\bar{t} + \gamma$, Drell-Yan and Di-

boson+ γ +jets. The contributions of $W\gamma$ +jets, W +jets, $t\bar{t}$ and $Z\gamma$ +jets events are all estimated from simulation as the SM background processes.

For the fully hadronic final state, the overwhelming QCD multijet backgrounds are large. We consider the main QCD backgrounds $jjjj$ and $bjjj$ for the signal state γjjb . However, the background could be significantly suppressed after a series of cuts.

We apply the basic selection cuts on the final states for two kinds of signals, γjjb and $\gamma l\nu b$. One of the distinctive signatures of the signal is the presence of a high- p_T photon in the final state. The photon is expected to carry large momentum because of the recoil against the heavy top quark. Photon candidates with significant energy are required to have transverse momentum $p_T \geq 50$ GeV with $|\eta| \leq 2.5$, using the CMS coordinate system presented [51]. Only jets with $p_T > 30$ GeV within $|\eta| \leq 2.5$ are considered in our analysis. Additionally, the particle flow isolation $\Delta R = \sqrt{(\Delta\eta)^2 + (\Delta\phi)^2} < 0.4$ around the photon candidate is applied, where $\Delta\eta$ is the rapidity gap and $\Delta\phi$ is the azimuthal angle gap between the particle pair. These cuts on photon insure the events with exactly one photon candidate. In order to have well separated physical objects and remove radiated photons from high p_T leptons or final state partons, it is required that $\Delta R(\text{jet}, \gamma) > 0.7$ and $\Delta R(\text{lepton}, \gamma) > 0.7$. The isolation criteria are corrected for the effects of pile-up and underlying events, and more details can be found in [38].

The average efficiency of single photon reaches 91%, and the probability for jets to reconstruct a single photon candidate in the electromagnetic calorimeter is about 0.1% [52]. To distinguish between b -jets and light flavor jets, b -tagging algorithm is used with the efficiency of about 70%. The misidentification probability of light quarks or gluons as b -jets is approximately 1.5%, which is given by the CMS collaboration [53].

In order to simulate signal and background events more realistically at the parton level, we imitate the experimental conditions with the Gaussian resolution parametrization smearing of the lepton (l), photon (γ) and jet (j) energies

$$\frac{\delta(E)}{E} = \frac{a}{\sqrt{E/\text{GeV}}} \oplus b, \quad (11)$$

where $\delta(E)/E$ is the energy resolution, a is a sampling term, b is a constant term, and \oplus denotes a sum in quadrature. We take $a = 5\%$, $b = 0.55\%$ for leptons and photons, $a = 100\%$, $b = 5\%$ for jets[54]. For simplicity we assume that the energy smearing for muon is the same as electron.

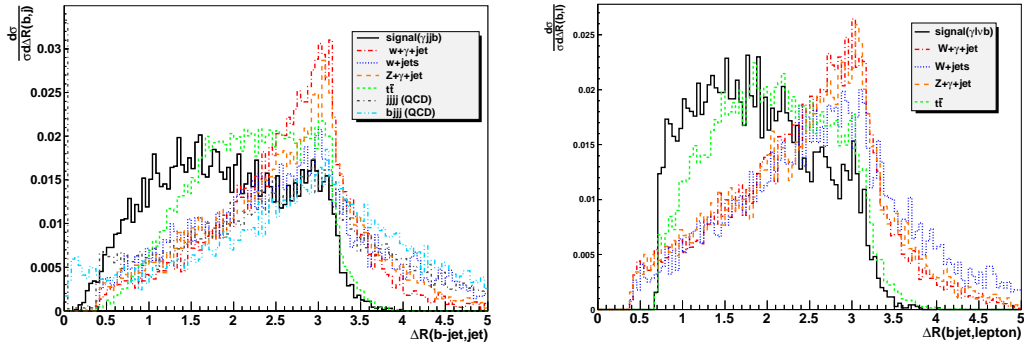


FIG. 3: Normalized ΔR distributions for γjjb (left) and $\gamma \ell \nu b$ (right) after the basic cuts and smearing at LHC-RunII.

Although the photon and b -jet p_T cut have good separation power to reduce the effect of soft jets from underlying events and pile-up, we also need other variables to reduce hard process backgrounds. The angular separation ΔR between the b -jet and lepton (or jet) could distinguish signal from backgrounds. It shows whether the W and b -jet, the former decay into jet or lepton, come from the same particle (top). So we display the distribution of $\Delta R(b\text{-jet}, \text{jet})$ for γjjb and $\Delta R(b\text{-jet}, \text{lepton})$ for $\gamma \ell \nu b$ in Fig.3. It is gratifying that this variable can partly discriminate between signal and the $t\bar{t}$ background events, although b -jet and lepton (or jet) are from the same one. In $t\bar{t}$ events, if the fake photons take the same p_T as the photons in signal, \bar{t} will carry more energy than signal photon. The momentum of the other top quark in $t\bar{t}$ events should be smaller than that of signal top quark, causing angular separation between the top quark decay products larger in $t\bar{t}$ backgrounds than that in signal. From Fig.3, we find $\Delta R(b\text{-jet}, \text{jet})$ and $\Delta R(b\text{-jet}, \text{lepton})$ should be less than 2.5 as one of the kinematical cuts.

In the following discussion, we employ other kinematical cuts, the mass windows of reconstructed W and top quark, to reduce backgrounds to a controlled level for γjjb and $\gamma \ell \nu b$.

1. The γjjb signal

The hadronic W decay is the main decay channel. Thus, although the leptonic W decay can give a more clean signal, the γjjb signal is also worth of pondering.

For the same final state of signal, one light jet need to be misidentified in the $W\gamma$ +jets, $Z\gamma$ +jets background events, and two jets in W +jets. If there is any jet more than these, the extra ones should be missed by a small p_T . However, there is no neutrino in the signal but missing energy (extra jets) in backgrounds. The events with extra jets could be well cut by the missing transverse momentum \cancel{E}_T or jet number. In our discussion, we only consider the background events with no extra jet for γjjb .

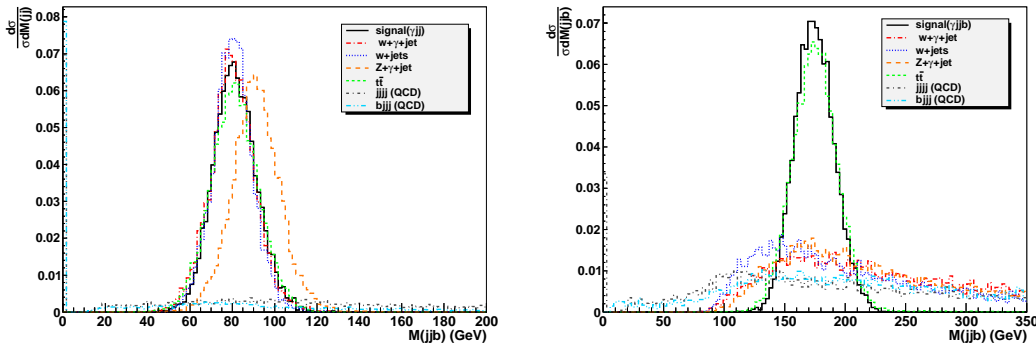


FIG. 4: Normalized $m(jj)$ (left) and $m(jj b)$ (right) distributions before the kinematical cuts for γjjb signal at LHC-RunII.

After basic cuts, we illustrate the distribution of reconstructed W mass for the γjjb signal and backgrounds at 14 TeV in Fig.4. From the left figure, it is evident that a proper mass window of W rapidly reduces the $Z\gamma$ +jets backgrounds while affecting the signal slightly. However, for $W\gamma$ +jets, W +jets or $t\bar{t}$, due to the same origin of two jets as the signal, the invariant mass $m(jj)$ alone is weak and ineffective to distinguish signal from backgrounds. Therefore, we subsequently reconstruct the top mass of two jets and a b -jet to further suppress backgrounds. The right one in Fig.4 shows a sharp peaky distribution for signal and the $t\bar{t}$ background with a maximum close to the top mass, while the other background events distribute in a broad invariant mass region. The difference is due to the b -jets in the W +jets, $W\gamma$ +jets and $Z\gamma$ +jets backgrounds coming from misidentified jets which makes the invariant mass $m(jj b)$ smaller than m_t .

In order to reduce backgrounds, we require the invariant mass of the two jets to peak at the W mass within a mass window of 15 GeV, as the following range,

$$|m(jj) - m_W| < 15 \text{ GeV}, \quad (12)$$

and further require the invariant mass $m(jjb)$ to be around the top quark mass window,

$$|m(jjb) - m_t| < 25 \text{ GeV}. \quad (13)$$

The cuts in Eq.11 and Eq.12 can reduce almost 80% W +jets, $W\gamma$ +jets and $Z\gamma$ +jets background events and nearly 20% signal and $t\bar{t}$ background events. As previously discussed, the $t\bar{t}$ is well cut by the $\Delta R(b\text{-jet,lepton})$ requirement. So we apply $\Delta R(b\text{-jet,lepton}) < 2.5$. Then we take into account the b -tagging efficiency and mistagging rates. After these event selection, the cross sections for the γjjb signal and backgrounds are listed in Table II with the same parameter value as before. It is obvious that our scheme of event selection can significantly suppress backgrounds.

TABLE II: The cross sections (in units fb) and the event numbers for the γjjb (signal and $W\gamma$ +jets, W +jets, $t\bar{t}$ and $Z\gamma$ +jets backgrounds) at LHC-RunII with $\mathcal{L} = 100\text{fb}^{-1}$.

	Signal γjjb	Bkg $W\gamma$ +jets	Bkg W +jets	Bkg $t\bar{t}$	Bkg $Z\gamma$ +jets	Bkg $jjjj$ (QCD)	Bkg $bjjj$ (QCD)
Basic cuts	12.87	1564.92	9.59×10^5	4651.56	924.85	2.51×10^9	2.88×10^7
After tag efficiency	8.11	21.13	14.39	3.26	12.49	37604	20179.8
$65\text{GeV} < m_{jj} < 95\text{GeV}$	7.7	20.20	13.71	2.98	9.84	4333.4	2750.2
$ m_{jjb} - m_t < 25\text{GeV}$	6.84	4.33	3.17	2.57	2.47	789.4	604.1
$\Delta R(b\text{-jet, jet}) < 2.5$	5.4	2.35	0.54	1.23	1.08	403.5	294.76
Number of events	540	234.5	54	123	108	40350	29476
$S/\sqrt{S+B}$	2.03						

We define the statistical significance (SS) as $S/\sqrt{(S+B)}$ where S and B denote the number of the signal and background events, respectively. For our coupling constants hypothesis, it gives a statistical significance of 2.03 at LHC-RunII with an integrated luminosity of 100 fb^{-1} . In section III, we will discuss the sensitivity of anomalous top couplings for this signal in detail.

2. The $\gamma\ell\nu b$ signal

The signal events are in general characterized by the presence of an isolated charged leptons (electrons or muons) together with a photon, missing transverse energy, and one b -jet. Although the production cross section for this signal is smaller than γjjb , the presence of lepton and photon provides a clean signal, which is attractive from the experimental

point of view. Moreover, $(\sigma(\ell^+)/\sigma(\ell^-))$ can be used to determine whether $t\gamma$ production comes from the up quark or charm quark initiated process [26, 55]. It provides the opportunity to understand the underlying new physics.

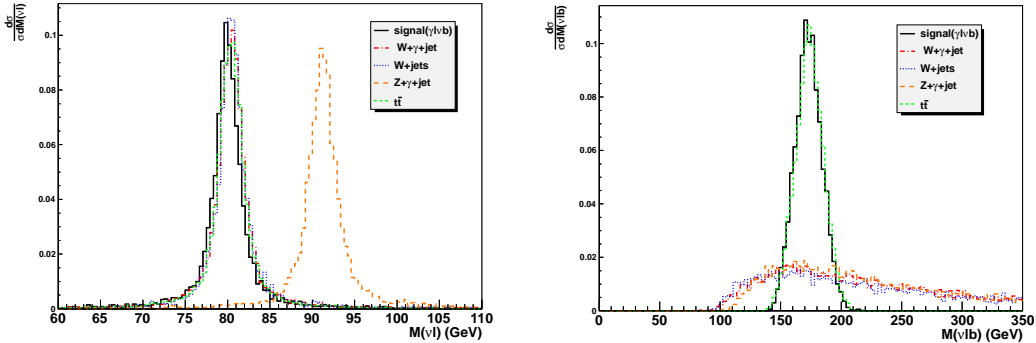


FIG. 5: Normalized $m(l\nu)$ and $m(l\nu b)$ distributions for the $\gamma l\nu b$ signal at LHC-RunII.

Events are preselected by requiring exactly the isolated charged leptons with a transverse momentum $p_T \geq 20$ GeV and a pseudorapidity $|\eta| \leq 2.5$. For the leptons, we only consider an electron and a muon in the signal simulation. The lepton-tagging efficiency is about $\epsilon_l = 90\%$. The missing transverse momentum \cancel{E}_T is required to be greater than 30 GeV. The parameters of anomalous top couplings in Fig.5 are taken the same as the γjjb signal.

The lepton with neutrino in the $\gamma l\nu b$ signal comes from W boson decay. For $Z\gamma$ +jets background, one of the jets is reconstructed to a b -jet and the other(s) should be missed. Similarly, one daughter-lepton of Z needs to be missed. Because the lepton cut is $p_T \geq 20$ GeV, the transverse energy of the missing lepton is required to be smaller than 20 GeV. The missing transverse momentum should satisfy $\cancel{E}_T > 30$ GeV, which is reconstructed by one or more missing jets and one missing lepton. So there must be more than one jet in the final state of $Z\gamma$ +jets backgrounds. In view of the small tag efficiency, we only consider $Z\gamma jj$ and $Z\gamma jjj$ backgrounds.

The W mass window can rapidly reduce $Z\gamma$ +jets backgrounds while affecting the signal slightly. The normalized invariant mass distribution of the lepton and neutrino (missed jets for $Z\gamma$ +jets) with the basic cuts is shown in Fig.5 (left). In order to further suppress other backgrounds, we subsequently reconstruct the mass of the top, and the normalized invariant mass distribution of the $m(l\nu b)$ spectrum are shown in Fig.5 (right).

The invariant mass for signal and $t\bar{t}$ background show narrower peaky distributions, and the SM background events distribute in the broad invariant mass region as expected. From the Fig.5, we require invariant mass cuts as

$$|m(\ell\nu) - m_W| < 15 \text{ GeV}, \quad (14)$$

$$|m(\ell\nu b) - m_t| < 25 \text{ GeV}. \quad (15)$$

We take $\Delta R(b\text{-jet,lepton}) < 2.5$ to suppress backgrounds, especially for $t\bar{t}$ backgrounds. After event selection, the efficiencies of these cuts are shown in Table III. As shown in Table

TABLE III: The cross sections (in units fb) and the event numbers for the $\gamma\ell\nu b$ signal and $W\gamma$ +jets, W +jets, $t\bar{t}$ and $Z\gamma$ +jets backgrounds at LHC-RunII with $\mathcal{L} = 100\text{fb}^{-1}$.

	Signal $\gamma\ell\nu b$	Bkg $W\gamma$ +jets	Bkg W +jets	Bkg $t\bar{t}$	Bkg $Z\gamma$ +jets
Basic cuts	8.59	854.05	3.67×10^5	660.86	34.65
After tag efficiency	4.87	10.38	4.95	0.41	0.403
$E_T > 30\text{GeV}$	3.51	6.83	3.38	0.31	0.120
$65\text{GeV} < m_{\ell\nu} < 95\text{GeV}$	3.37	6.47	3.21	0.29	0.029
$ m_{\ell\nu b} - m_t < 25\text{GeV}$	3.28	1.43	0.68	0.28	0.023
$\Delta R(b\text{-jet,lepton}) < 2.5$	2.47	0.95	0.41	0.21	0.003
Number of events	247	95	41.4	21	0.3
$S/\sqrt{S+B}$	12.28				

III, the sets of cuts significantly suppress the backgrounds. The statistical significance can reach 12.28 at LHC-RunII with an integrated luminosity of 100fb^{-1} with the $\kappa_{tq\gamma}$ and κ_{tqg} corresponding to what mentioned earlier. There will be a detailed discussion about the sensitivity of anomalous top couplings in the next section.

C. The contribution of photon radiation to signal

For the signal of anomalous top couplings tqg , $t\gamma$ associated production is not the only contribution to γjjb and $\gamma\ell\nu b$. The additional feynman diagrams for $qg \rightarrow \gamma f\bar{f}b$ are depicted in Fig.6. They correspond to direct top production and photon radiation of the

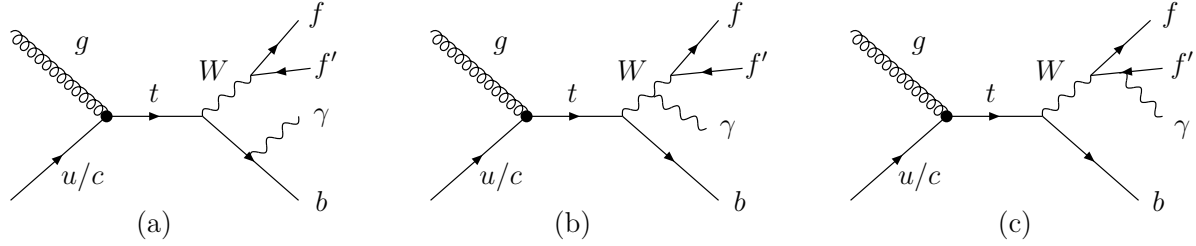


FIG. 6: Additional Feynman diagrams contributing to the signal of top decay products in association with a photon through tqg vertices.

b quark, W boson and W decay products, respectively. The existence of these processes allow to test whether it is induced by strong interactions. Therefore, it is a necessary probe to research the top-quark FCNC as a supplementary.

In [20], the author calculated the contributions of the radiation process to total cross sections which has not been taken into account in previous literature. But they only considered the transverse momentum cut on photon so that their conclusion is too optimistic. We take account of basic cuts on b -jet and lepton (or jet) to examine the contributions of the radiation process. By setting basic cuts and $p_T^\gamma > 15$, we present the cross sections of additional feynman diagrams with the strengths of anomalous top couplings in Fig.7.

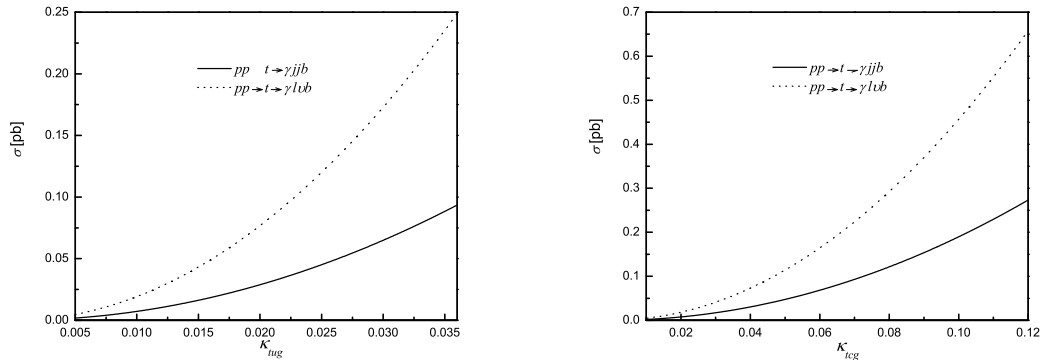


FIG. 7: The cross sections of the radiation process induced by couplings tug (left) and tcg (right) with $p_T^\gamma > 15$ GeV.

After setting our basic cuts, we note that this part of contributions to total cross section have a rapid decrease with the photon transverse momentum increasing. When $p_T^\gamma > 5$, for $\gamma j j b$ ($\gamma l \nu b$), the total cross section which contains the contributions of radiation processes

is doubling (tripling) of the $t\gamma$ production with subsequent top decay. When $p_T^\gamma > 40$, the contributions of additional feynman diagrams to the cross section quickly decrease to less than 10% of $t\gamma$ production with subsequent top decay. Thus we conclude that the contributions from $t\gamma$ production with subsequent top decay dominate in part of $p_T^\gamma > 50$. Nevertheless, the contributions from these additional feynman diagrams could help us to search for top FCNC process when relatively small transverse momentum cut on photon is imposed. In this case, it is necessary to consider not only the final states of a top quark plus a photon but also the final state particles reconstructing a top quark. Thus we present the normalized $m(f\bar{f}b)$ and $m(\gamma f\bar{f}b)$ distributions for the $\gamma f\bar{f}b$ in Fig.8.

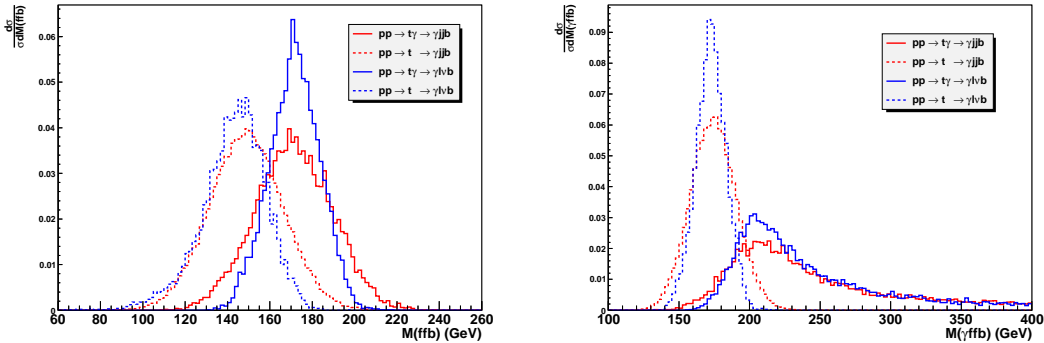


FIG. 8: Normalized $m(f\bar{f}b)$ (left) and $m(\gamma f\bar{f}b)$ (right) distributions for the $\gamma f\bar{f}b$ signals via different processes with $p_T^\gamma > 15$ GeV. The $f\bar{f}$ here denotes W decay products jj or $\ell\nu$.

III. SENSITIVITY OF ANOMALOUS TOP COUPLINGS AT LHC-RUNII

In this section, we study the sensitivity of anomalous couplings through the $t\gamma$ production at LHC-RunII. For an adequate signal modelling, the photon radiation from top quark decay products is taken into account. The sensitivity of four anomalous top couplings at LHC-RunII which is defined as $S/\sqrt{S+B}$ (as shown above) are presented in Fig.9. The SS is obtained with the selection strategy for high signal efficiency. In the case of assuming a single non-vanishing coupling at a time, four choices of anomalous coupling parameters are subsequently fitted by polynomial functions so that 3σ and 5σ discovery ranges are extracted. Assuming that LHC-RunII could collect an integrated luminosity

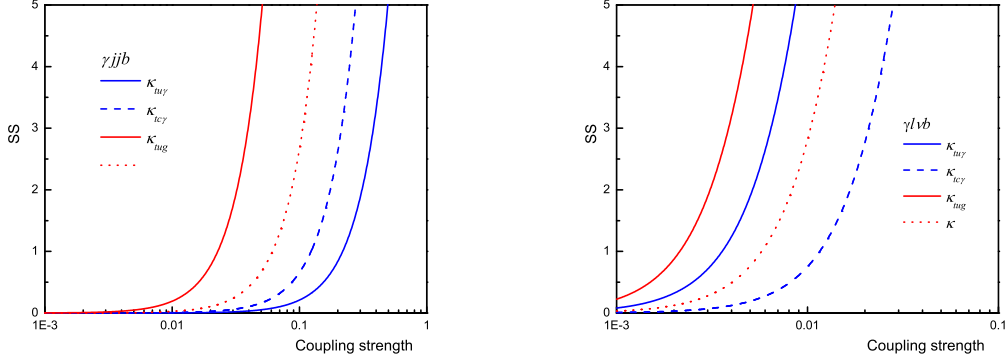


FIG. 9: LHC sensitivity to the considered anomalous top couplings as a function of the coupling strengths after applying the kinematical cuts and event selection.

of 100 fb^{-1} , we obtain the constraints of one-dimensional discovery limits of anomalous couplings as shown in Table IV.

TABLE IV: 5σ (3σ) discovery lower limits on top-quark FCNC anomalous couplings.

Signal	$\kappa_{tu\gamma}$	$\kappa_{c\gamma}$	κ_{tug}	$\kappa_{tc\gamma}$
γjjb	0.0851(0.0659)	0.2759(0.2137)	0.0510(0.0395)	0.1370(0.1061)
$\gamma l\nu b$	0.0086(0.0064)	0.0280(0.0209)	0.0052(0.0039)	0.0139(0.0103)

The limits on the strength of FCNC anomalous couplings can be converted to constraints on the branching ratios of rare top decays at the 5σ (3σ) levels and are summarized in Table V.

TABLE V: The 5σ (3σ) discovery lower limits on top-quark anomalous branching ratios.

Signal	$\mathcal{BR}(t \rightarrow u\gamma)$	$\mathcal{BR}(t \rightarrow c\gamma)$	$\mathcal{BR}(t \rightarrow ug)$	$\mathcal{BR}(t \rightarrow cg)$
γjjb	1.413×10^{-3} (8.473×10^{-4})	0.015 (0.009)	0.021 (0.013)	0.152 (0.091)
$\gamma l\nu b$	1.459×10^{-5} (8.095×10^{-6})	1.536×10^{-4} (8.519×10^{-5})	2.176×10^{-4} (1.207×10^{-4})	1.570×10^{-3} (8.711×10^{-4})

Obviously, the $\gamma l\nu b$ signal is more sensitive than γjjb . For hadronic final state, the overwhelming QCD multijet backgrounds make the FCNC coupling constants looser. Thus the $\gamma l\nu b$ is the better signal to search for anomalous couplings at LHC-RunII with an integrated luminosity of 100 fb^{-1} .

Actually, we allow for a set of non-vanishing couplings simultaneously, either in the weak sector (non-vanishing $\kappa_{tu\gamma}$ and $\kappa_{tc\gamma}$) or in the strong sector (non-vanishing κ_{tug} and

κ_{tcg}). In order to illustrate excluded detection potential regions of anomalous couplings to reach a given statistical significance, we plot the associated 3σ and 5σ discovery reaches in $\kappa_{tu\gamma}$ - $\kappa_{tc\gamma}$ (κ_{tug} - κ_{tcg}) planes for $\gamma\ell\nu b$ at LHC-RunII in Fig.10. We observe a better sensitivity to flavor-changing interactions with an up quark than with a charm quark, as expected from parton densities, the charm content of the proton being suppressed with respect to its up content.

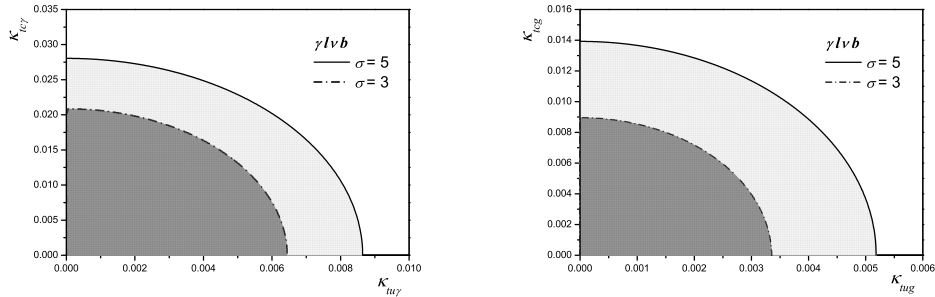


FIG. 10: Excluded 3σ and 5σ detection potential regions for the $\gamma\ell\nu b$ signal in weak (left) and strong (right) sector at LHC-RunII.

Since both $tq\gamma$ and tqg operators contribute to the same final state, the interference effects should be considered. If $\kappa_{tu\gamma} = \kappa_{tc\gamma} = \kappa_{tq\gamma}$, $\kappa_{tug} = \kappa_{tcg} = \kappa_{tqg}$, for $p_T^\gamma > 50$ GeV, the total $t\gamma$ cross section with contributions of $tq\gamma$ and tqg operators is

$$\sigma_{t\gamma} = 158.2 |\kappa_{tq\gamma}|^2 + 457.3 |\kappa_{tqg}|^2 + 153 \kappa_{tq\gamma} \cdot \kappa_{tqg} \text{ (pb)}. \quad (16)$$

By applying the same selection strategy described as above, we presented excluded LHC-RunII detection potential regions for the $\gamma\ell\nu b$ signal in $tq\gamma$ and tqg plane in Fig.11. Compared to existing researches about tZ production and same-sign top quark production[27, 32], our results give more sensitive constraints on top anomalous couplings via $t\gamma$ production.

IV. CONCLUSIONS

Many of the extensions of the SM predict that the tree level FCNC processes could exist. With Run-II of the LHC, more and more measurements in the top-quark sector will be explored with an unprecedented precision. Measurements of single top production

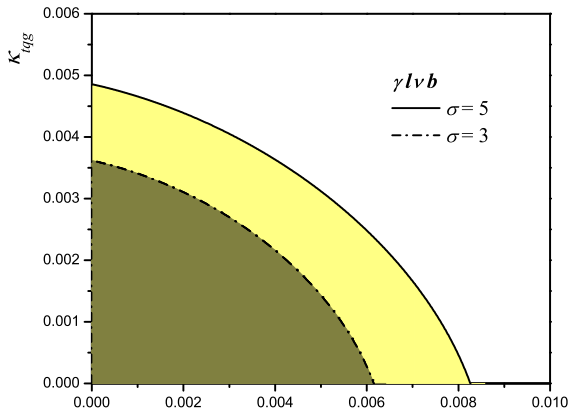


FIG. 11: Excluded region for 3σ and 5σ statistical significances at LHC-RunII in the $\kappa_{tq\gamma} - \kappa_{tqg}$ plane.

allow us to search for deviations from the SM predictions. While these deviations are often interpreted in terms of anomalous top couplings. The possible deviations can be described by the effects of effective operators, and experimental results can be used to determine useful constraints on each effective operator. The established deviations can then be evolved up to high scales, and matched to possible new physics scenarios.

In this paper, we have investigated FCNC couplings $tq\gamma$ and tqg in a model independent way. These interactions lead to possibly significant production rates for γjjb and $\gamma l\nu b$ signals via $t\gamma$ associated production with subsequent decay. We have considered the contribution of the single top production with photon radiation off the top decay products to this process. This contribution dominate when p_T^γ is small, and it quickly decrease with the photon transverse momentum increasing. For the cuts we took here, as the CMS and ATLAS experiments presented, the contribution of this process has little effect on the results. While for smaller p_T^γ cut, this process could be useful. Once $t\gamma$ production processes are eventually observed, the single top decay with photon radiation processes could help us find out whether or not the origin of the FCNC interactions is in the strong sector.

We systematically considered various experimental requirements for our basic cuts. Meanwhile, we employed the lepton, photon and b -tag efficiencies on signal and back-

ground predictions to improve the results. By using the sequential cuts and event selection, a detailed analysis of reconstruction and invariant mass distribution was performed to improve the statistical significance. Moreover, the sensitivities of LHC-RunII to anomalous FCNC couplings $tq\gamma$ and tqg were calculated for both the γjjb and $\gamma \ell \nu b$ signals. We further discussed the interference effects on the cross section from contributions of $tq\gamma$ and tqg operators. Then we presented excluded detection potential regions for the $\gamma \ell \nu b$ signal. With an integrated luminosity of 100 fb^{-1} and $\sqrt{s} = 14 \text{ TeV}$, for a 5σ discovery, the needed strengths of $tq\gamma$ and tqg couplings of order are down to 0.001-0.01. Equivalently, the lower bounds on the associated rare top branching ratios are $\mathcal{O}(0.001 - 0.1)\%$ which are one order of magnitude tighter than the ones from LHC experiments. We hope our results could help search for the signal of anomalous top couplings at LHC-RunII in operation.

Acknowledgement

One of us (Y. C. G.) acknowledge illuminating discussions with Celine Degrande, Cen Zhang, Eric Conte on the analysis of reconstruction at MadGraph School Shanghai 2015. Y. C. G. would like to thank Jian Wang for reading the manuscript and valuable discussions. This work was supported in part by the National Natural Science Foundation of China under Grants No.11275088, No.11175251, and No.11205023, the Natural Science Foundation of the Liaoning Scientific Committee (No.2014020151) and Liaoning Excellent Talents in University (Grant No.LJQ2014135).

-
- [1] W. Bernreuther, J. Phys. G **35**, 083001 (2008).
 - [2] S. L. Glashow, J. Iliopoulos, and L. Maiani, Phys. Rev. D **2**, 1285 (1970).
 - [3] J. A. Aguilar-Saavedra and B. Nobre, Phys.Lett. B **553**, 251 (2003).
 - [4] J. A. Aguilar-Saavedra, Acta Phys. Polon. B **35**, 2695 (2004).
 - [5] G. Couture, M. Frank, and H. Konig, Phys. Rev. D **56**, 4213 (1997).
 - [6] G. R. Lu, F. R. Yin, X. L. Wang, and L. D.Wan, Phys. Rev. D **68**, 015002 (2003).
 - [7] J. A. Aguilar-Saavedra, Phys. Rev. D **67**, 035003 (2003).

- [8] M. E. Luke, M.J. Savage, Phys. Lett. B **307**, 387 (1993).
- [9] S. Bejar, J. Guasch, J. Sola, Nucl. Phys. B **600**, 21 (2001).
- [10] J. M. Yang, B.-L. Young, X. Zhang, Phys. Rev. D **58**, 055001 (1998).
- [11] D. Delepine, S. Khalil, Phys. Lett. B **599**, 62 (2004).
- [12] J. J. Liu, *et al.*, Phys. Lett. B **599**, 92 (2004).
- [13] J. J. Cao, *et al.*, Phys. Rev. D **75**, 075021 (2007).
- [14] M. Beneke *et al.*, Report No. CERN-TH/2000-100 (2000).
- [15] J. M. Yang, Int. J. Mod. Phys. A **23**, 3343 (2008).
- [16] J. A. Aguilar-Saavedra, Nuclear Physics B **812**, 181 (2009).
- [17] F. del Aguila, J. A. Aguilar-Saavedra, Nucl.Phys. B **576**, 56 (2000).
- [18] J. J. Zhang, C. S. Li, J. Gao, H. Zhang, Z. Li, C.-P. Yuan, T.-C. Yuan, Phys.Rev.Lett. **102**, 072001 (2009).
- [19] J. Gao, C. S. Li, J. J. Zhang, H. X. Zhu, Phys.Rev.D **80**, 114017 (2009).
- [20] J. A. Aguilar-Saavedra, Nucl.Phys.B **837**, 122 (2010).
- [21] J. Drobnak, S. Fajfer, J. F. Kamenik, Phys.Rev.Lett. **104**, 252001 (2010)
- [22] J. J. Zhang, C. S. Li, J. Gao, H. X. Zhu, C.-P. Yuan, T.-C. Yuan, Phys.Rev.D **82**,073005 (2010).
- [23] J. Drobnak, S. Fajfer, J. F. Kamenik, Phys.Rev.D **82**,073016 (2010)
- [24] Y. Zhang, B. H. Li, C. S. Li, J. Gao, H. X. Zhu , Phys.Rev.D **83**, 094003 (2011).
- [25] B. H. Li, Y. Zhang, C. S. Li, J. Gao, H. X. Zhu, Phys.Rev.D **83**, 114049 (2011)
- [26] J. Gao, C. S. Li, L. L. Yang, and H. Zhang, Phys. Rev. Lett. **107**, 092002 (2011).
- [27] J. Agram, J. Andrea, E. Conte, B. Fuks et al., Phys. Lett. B **725** 123 (2013).
- [28] D. Atwood, S. K. Gupta, and A. Soni, J. High Energy Phys.**1410**, 57 (2014).
- [29] C. Zhang, Fabio Maltoni, Phys. Rev. D **88**, 054005 (2013)
- [30] C. Zhang, Phys. Rev. D **90**, 014008 (2014)
- [31] H. Sun, Nucl.Phys. B **886**, 691 (2014).
- [32] R. Goldouzian, Phys. Rev. D **91**, 014022 (2015).
- [33] C. Degrande, F. Maltoni, J. Wang, C. Zhang, Phys.Rev.D **91**, 034024 (2015).
- [34] G. Durieux, F. Maltoni, C. Zhang, Phys. Rev. D **91**, 074017 (2015).
- [35] S. Khatibi, M. Mohammadi Najafabadi, arXiv:1511.00220 [hep-ph].

- [36] O. Bessidskaia Bylund, F. Maltoni, I. Tsirikos, E. Vryonidou, C. Zhang, Report No. CP3-16-03, MCnet-16-03 (2016), arXiv:1601.08193 [hep-ph].
- [37] D. Bardhan, G. Bhattacharyya, D. Ghosh, M. Patra, S. Raychaudhuri, Report No. TIFR-TH/16-02 (2016), arXiv:1601.04165 [hep-ph].
- [38] CMS Collaboration, Report No. CMS-TOP-14-003, CERN-PH-EP-2015-287 (2014). arXiv:1511.03951 [hep-ex]
- [39] CMS Collaboration, Report No. CMS PAS TOP-14-007 (2014).
- [40] J. Pumplin, D. Stump, J. Huston, and *et al.*, J. High Energy Phys. **07**, 012 (2002).
- [41] A. Alloul, N. D. Christensen, C. Degrande, C. Duhr, B. Fuks, J.Phys.Conf.Ser. **523**, 012044 (2014).
- [42] J. Alwall, M. Herquet, F. Maltoni, O. Mattelaer, and T.Stelzer, J. High Energy Phys. **06**, 128 (2011).
- [43] C. Degrande, C. Duhr, B. Fuks, D. Grellscheid, O. Mattelaer, and T. Reiter, Comput. Phys. Commun **183**, 1201 (2012).
- [44] J. A. Aguilar-Saavedra, Acta Phys.Polon.B **35** 2695 (2004)
- [45] CDF Collaboration, Phys. Rev. Lett. **80**, 2525 (1998).
- [46] CDF Collaboration, Phys. Rev. Lett. **102**, 151801 (2009).
- [47] D0 Collaboration, Phys. Lett. B **693**, 81 (2010).
- [48] CMS Collaboration, Report No. CMS-PAS-TOP-12-021 (2012).
- [49] ATLAS Collaboration, Report No. ATLAS-CONF-2013-063 (2013).
- [50] G. Aad *et al.* (ATLAS Collaboration), Phys.Lett. B **712**, 351 (2012).
- [51] G. Bayatian *et al.* (CMS Collaboration), J.Phys. G **34**, 995 (2007).
- [52] CMS Collaboration, CMS NOTE -2006/007 (2006).
- [53] CMS Collaboration, Report No. CMS-PAS-BTV-13-001 (2013).
- [54] G. Aad *et al.*, (ATLAS Collaboration). arXiv: 0901.0512.
- [55] S. Khatibi and M. Mohammadi Najafabadi, Phys. Rev. D **89**, 054011 (2014).